CHAPTER 64

BREAKPOINT-FORCED AND BOUND LONG WAVES IN THE NEARSHORE: A MODEL COMPARISON

JEFFREY H. LIST

U.S. Geological Survey, 600 4th St. S., St. Petersburg, FL 33701 U.S.A.

ABSTRACT

A finite-difference model is used to compare long wave amplitudes arising from two group-forced generation mechanisms in the nearshore: long waves generated at a time-varying breakpoint and the shallow-water extension of the bound long wave. Plane beach results demonstrate that the strong frequency selection in the outgoing wave predicted by the breakpoint-forcing mechanism may not be observable in field data due to this wave's relatively small size and its predicted phase relation with the bound wave. Over a bar/trough nearshore, it is shown that a strong frequency selection in shoreline amplitudes is not a unique result of the time-varying breakpoint model, but a general result of the interaction between topography and any broad-banded forcing of nearshore long waves.

INTRODUCTION

Recent observations have shown that long period (30-300 sec.) waves often dominate the wave energy spectrum near the shoreline, especially during storms and on dissipative beaches. Despite the evident importance of these low frequency oscillations, also known as infragravity waves, much work is needed to understand the mechanisms by which these waves are generated. This paper concerns the generation of one form of these waves—the leaky modes, normally or near-normally incident long waves whose energy is radiated seaward after shoreline reflection.

Two primary models have been proposed for the generation of leaky modes, both of which depend on forcing by incident wave groupiness. Longuet-Higgins and Stewart (1962) showed that radiation stress gradients in unbroken wave groups force a second-order sea-surface fluctuation in the form of a phase-locked or bound long wave. Although this concept has been substantiated in both field and laboratory observations (Sand, 1982; Kostense, 1985), it is clear that bound wave theory is not applicable in very shallow water where the Ursell number is large (Longuet-Higgins and Stewart, 1964, Okihiro et al., 1992).

Symonds et al. (1982) proposed an alternate model for leaky mode generation in which incident wave groups produce a forcing region associated with the time-varying position of the breakpoint. This model predicts a characteristic frequency selection in the amplitudes of the outgoing (seaward propagating) long waves. While substantiated by one laboratory experiment (Kostense, 1985), this frequency selection has never been observed in spectra calculated from field data. With an extension to a bar/trough topography, the time-varying breakpoint model also predicts a strong frequency selection in shoreline amplitudes (Symonds and Bowen, 1984), suggesting a resonant phenomenon. However, it has remained unclear whether this apparent resonance is a direct result of the time-varying breakpoint forcing, or just a natural outcome of the interaction between a bar/trough topography and any broad-banded long wave forcing.

In this study, a numerical scheme (List, 1988b, 1992) is used to investigate the relative magnitudes of the breakpoint-forced long wave (hereafter BFLW) and bound long wave (BLW), as well as the specific predictions of the breakpoint-forcing model described above.

MODEL FORMULATION AND RUN PARAMETERS

List (1988b,1992) constructed a finite-difference solution to the equations of cross-shore (x-directed) continuity and momentum given by

$$\frac{\partial \eta}{\partial t} + \frac{\partial (hu)}{\partial x} = 0 \tag{1}$$

$$\frac{\partial u}{\partial t} + g\frac{\partial \eta}{\partial x} = -\frac{1}{\rho h}\frac{\partial Sxx}{\partial x} \tag{2}$$

where η and u are the time-averaged (over the incident wave period) sea-surface and vertically-integrated cross-shore current respectively, h is the water depth, and Sxx is the radiation stress in the cross-shore direction. An incident waves model provided non-steady Sxx gradients in both broken and unbroken waves through the surf zone over arbitrary topography. Incident waves were modeled as the wave envelope, which progressed over the bottom topography at the shallow water phase speed, shoaling and breaking as a function of the water depth. Long waves were generated throughout the nearshore by both the time-varying breakpoint and bound wave mechanisms. Long waves were reflected from a vertical wall near the shoreline, where the depth is $\geq$ the long wave amplitude. This mode of shoreline reflection crudely approximates natural reflection from a sloping beach, though the position of the shoreline is shifted seaward. (Although the depth at the reflection point can be a large fraction of the long wave amplitude, the model does not permit breaking.) Following shoreline reflection, waves propagate seaward and exit from the model through a radiative boundary condition. Support for the model came from an accurate simulation of the cross-correlation signal between groups and long waves from random wave records both inside and outside a natural surf zone. Key to the present study, a means of separating the BFLW and BLW components was demonstrated in which the model is run separately with BFLW forcing only, BLW forcing only, or total combined forcing.

Here, the model is run with both a plane beach (slope $\tan\beta = 0.025$, Fig. 2) and the idealized bar/trough topography of Symonds and Bowen (1984) (Fig. 3). Incident waves, again parameterized as the wave envelope, enter the model at depth $h = 15$ m, requiring a minor extension to the model described above to allow for intermediate-depth phase speeds for wave groups. Model runs are conducted at a series of discrete group frequencies defined by the beating of incident wave pairs (Table 1). Except for runs generating only the BFLW, an incoming BLW at the boundary was specified following Ottesen Hansen et al. (1981). As shown in Table 1, this gives an input BLW magnitude that is almost negligible compared to long wave amplitudes generated by the model in shallower water.

For the plane beach case, the model was run with a distance step $\Delta x = 7.5$ m, a time step $\Delta t = 0.5$ sec., and a shoreline reflection depth $h_o = 0.49$ m. Plane beach results other than for the conditions reported in Table 1 are given by List (1988b). For the bar/trough case, the model was run with $\Delta x = 5.0$ m, $\Delta t = 0.25$ sec., and $h_o = 0.26$ m. The different choice of parameters for the bar/trough case was related to geometric constraints; as discussed by List (1992), the choice of time step has no significant influence on the results. Other model parameters were the same as used by List (1992).

Wave amplitudes reported below were found from model-generated time series of a length of at least one group period, T_g, after an initial interval for model stabilization. For the plane beach results, amplitudes were found from the interval $t = 200 \rightarrow 400$ sec., while for the bar/trough results amplitudes were found from $t = 700 \rightarrow 900$ sec.; the need for a much later start time for the bar/trough case will become apparent below.

RESULTS

Plane Beach

Figure 1A gives the amplitude of the long waves at the shoreline ($h_o = 0.49$ m reflection point) for model runs in BFLW, BLW and total forcing modes for the plane beach case. Except at the lowest frequencies, the BLW is predicted to be larger than the BFLW. Interestingly, the long waves generated in total forcing mode are lower at all frequencies than the sum of the BFLW and BLW. There is also a systematic variation in the degree to which the sum of the BFLW and BLW is destructive, with the total solution being less than either the BFLW or BLW at low frequencies, while at high frequencies the total solution amplitude is nearly identical to the BLW. An investigation of the phase between the envelope, $A(t)$, and the BLW seaward of the surf zone as well as between the BFLW and BLW near the shoreline, shown in Fig. 2, explains this model result. As the BLW progresses into shallow water, it lags behind the group structure, with higher frequencies showing a greater departure from the deepwater 180° relationship with $A(t)$. Higher frequencies are then closer to a 90° relation with the BFLW in the surf zone, resulting in a less destructive interference. This lag of the BLW behind $A(t)$ has been shown previously by Elgar and Guza (1985) and List (1992).

Figure 1B shows the amplitude of the outgoing sea-surface component, $\eta(off)$, found by separating the onshore ($\eta(on)$) and offshore ($\eta(off)$) progressive long wave components following Guza et al. (1985). Model results are again shown for runs in BFLW, BLW, and total forcing modes, with the BLW now a free long wave after shoreline reflection. The BFLW clearly shows the frequency selection predicted by Symonds et al. (1982). The amplitude of the total solution relative to the BFLW and BLW indicates a highly variable phase relation between the BFLW and BLW for these outgoing waves. However, the net result is that the total solution amplitudes do not show a distinctive structure, apart from a general increase with increasing frequency.

Bar/Trough Nearshore

Figure 4 gives the amplitude of the long waves at the shoreline ($h_o = 0.26$ m reflection point) for model runs in BFLW, BLW and total forcing modes over the bar/trough profile of Symonds and Bowen (1984) (Fig. 3). While the overall trends are similar to the plane beach case (Fig. 1A), there are now marked peaks at $f_g = 0.0172$ Hz and $f_g = 0.0309$ Hz for all forcing modes. Except for a frequency shift in the peaks due to a shoreline reflection point with $h_0 > 0$, the structure is almost identical to that predicted by Symonds and Bowen (1984). The most striking result in Fig. 4 is that the shallow water bound wave is just as likely to force the distinctive set of shoreline peaks as the breakpoint-forcing mechanism.

Because the above results suggested that the forcing mode is irrelevant to the generation of the peaked amplitude spectrum, a test was conducted in which all incident wave forcing was turned off, leaving only the solution to eqns. (1) and (2) with a small input long wave of variable frequency. For Figs. 5 and 6 the model was run in this mode at a series of discrete frequencies with $\Delta x = 5.0$ m, $\Delta t = 0.5$ sec, and an incoming long wave at $x = 400.0$ m ($h = 5.2$ m, Fig. 3) with amplitude $A = 0.01$ m for all frequencies. Shoreline amplitudes were found at a reflection point with $h_0 = 0.1$ m. These parameters were changed from the forcing-inclusive runs to improve model efficiency; the qualitative interpretation of the results is unaffected.

With the model configured in this way, the peaked shoreline amplitude structure is reproduced once more, as shown in Fig. 5 ($t = 700$ sec. curve). (Note that the peak frequencies are again shifted due to a different depth of shoreline reflection, h_o.) This demonstrates that the Symonds and Bowen (1984) result can be reproduced by any model that generates a white spectrum of long waves incident to a bar/trough nearshore.

Symonds and Bowen (1984) suggested that these peak frequencies satisfy a "half-wave resonance" condition, in which an antinode in η corresponds with the bar crest. The characteristics of this potential resonance are investigated here by examining the time development of the amplitude structure. Fig. 5 shows long wave amplitudes found from group period length intervals starting at two different times: $t = 110$ sec., or just after input long waves have reached the shoreline, and $t = 700$ sec. after time for model stabilization. Except at the lowest frequencies, the amplitude of the $t = 110$ sec. curve is almost invariant with frequency, at a level of about 0.05 m. This is the expected value for the shoreline amplitude of a standing wave, given shoaling of the $A = 0.01$ m input wave from $h = 5.2$ m to $h = 0.1$ m. After 700 seconds there is a strong amplitude increase at the "half-wave resonance" frequencies, supporting the concept that these frequencies represent a resonant condition.

However, two other observations complicate this otherwise straightforward interpretation of a resonant phenomenon. First, as shown in Fig. 5, the non-resonant frequencies actually decrease in amplitude over time. Although this was also seen by Symonds and Bowen (1984) in a comparison between their bar/trough and plane beach results, the reason for this model result is not known. Second, the model as formulated using eqns. (1) and (2) contains no term for frictional dissipation; "resonant" peaks should continue to grow in amplitude until model depth limits are exceeded. However, as shown in Fig. 6, this is not the case; with time, peak and valley amplitudes reach a stable value. List (1988a) predicted the same shoreline structure using leaky mode solutions over the Symonds and Bowen profile, suggesting that the peak/valley result relates more to an uneven distribution of wave energy across the nearshore than to a true resonance.

DISCUSSION

The prediction of a strong, apparently linear, dependence of the BLW magnitude on the group frequency, shown in Fig. 1A, may be an artifact of the model simplifications, especially the lack of an energy balance between short and long waves. Field observations do not in general support this result. More recent models (e.g. Roelvink, 1991; Roelvink et al., this volume; Watson and Peregrine, this volume) may address this problem, although these models have not yet been directly tested in this respect. Thus the model result that the total outgoing wave will not show a distinctive frequency selection, as predicted by Symonds et al. (1982), is tempered by this problem.

In fact, some laboratory data do show a frequency selection in the outgoing wave (Kostense, 1985); this same pattern is reproduced, at least qualitatively, by the model of Roelvink et al. (this volume). However, modeling of a field data set (List, 1992) suggests that the BLW can be much larger than the BFLW, at least under certain conditions. In this case the outgoing long wave will not show a strong frequency selection. Consistent with this is the lack of supporting field observations showing a strongly peaked spectrum in the long waves offshore, despite a decade of nearshore field experiments since the Symonds et al. (1982) prediction. The results presented in this paper suggest that while the breakpoint-forcing mechanism may be valid and operative, the wave generated by this means has an amplitude and phase relation to the BLW such that a frequency selection in the outgoing wave will not be strong, explaining the lack of this type of field observation.

Although the bar/trough results clearly show that any white long wave forcing can result in a distinctly-peaked elevation spectrum at the shoreline, an explanation of this result as a resonant phenomenon, as suggested by Symonds and Bowen (1984), is subject to questions concerning the mechanism for lowering the amplitudes at non-resonant frequencies and for limiting the overall response. Clearly more work is needed to understand the nature of this interaction between topography and long wave dynamics.

CONCLUSIONS

A possible explanation for the lack of field observations showing a strong frequency selection in the seaward propagating long waves, as predicted by the Symonds et al. (1982) model, is proposed. The breakpoint-forced long wave's relatively small size and phase relation with the wave originating as a bound wave may preclude this observation.

It is also shown that a strongly peaked elevation spectrum at the shoreline in the presence of a bar/trough topography (Symonds and Bowen, 1984) is not a unique result of the time-varying breakpoint model. It is demonstrated that any white forcing of long waves incident to a bar/trough nearshore can produce this result. Accounting for this frequency selection as a resonant phenomenon will require an explanation of several unusual observations related to the time development of this peak/valley structure.

ACKNOWLEDGEMENTS

Karen Monroe is thanked for preparing the figures. This study began at the Virginia Institute of Marine Science, Gloucester Point, Virginia, where L.D. Wright is thanked for encouraging and supporting this work.

REFERENCES

Elgar, S., and R.T. Guza, 1985, Observations of bispectra of shoaling surface gravity waves, J. Fluid Mech., 161, 425-448.

Guza, R.T., Thornton, E.B., and Holman, R.A., 1985, Swash on steep and shallow beaches, Proceed. 19th Internat. Conf. Coastal Eng., ASCE, 708-723.

Kostense, J.K., 1985, Measurements of surf beat and set-down beneath wave groups, Proceed. 19th Internat. Conf. Coastal Eng., ASCE, 724-740.

List, J.H., 1988a, Leaky mode simulations over a bar-trough nearshore, Abstracts, AGU Fall Meeting, EOS Transactions, v. 69, n. 44, p. 1248.

List, J.H., 1988b, Long wave generation by wave groups in the nearshore, Ph.D. Dissertation, Virginia Institute of Marine Science, Gloucester Point, Virginia.

List, J.H., 1992, A model for two-dimensional surf beat, J. Geophys. Res., 97, 5623-5635.

Longuet-Higgins, M.S., and Stewart, R.W., 1962, Radiation stress and mass transport in gravity waves, with application to surf beats, J. Fluid Mech., 13, 481-504.

Longuet-Higgins, M.S., and Stewart, R.W., 1964, Radiation stress in water waves: a physical discussion, with applications, Deep Sea Res., 11, 529-562.

Okihiro, M., Guza, R.T., and Seymour, R.J., 1992, Bound infragravity waves, J. Geophys. Res., 92, 11453-11469.

Ottesen Hansen, N.-E., Sand, S.E., Lundgren, H., Sorensen, T., and Gravesen, H., 1981, Correct reproduction of group-induced long waves, Proceed. 17th Internat. Conf. Coastal Eng., ASCE, 784-800.

Roelvink, J.A., 1991, Modeling of cross-shore flow and morphology, Proceed. Coastal Seds '91, ASCE, 603-617.

Roelvink, J.A., Petit, H.A.H., and Kostense, J.K., 1993, Verification of a one-dimensional surfbeat model against laboratory data, this volume.

Sand, S.E., 1982, Long wave in directional seas, Coastal Eng., 6, 195-208.

Symonds, G., Huntley, D.A., and Bowen, A.J., 1982, Two-dimensional surf beat: long wave generation by a time-varying breakpoint, J. Geophys. Res., 87, 492-498.

Symonds, G., and Bowen, A.J., 1984, Interactions of nearshore bars with incoming wave groups, J. Geophys. Res., 89, 1953-1959.

Watson, G., and Peregrine, D.H., 1992, Low frequency waves in the surf zone, this volume.

			Plane Beach Profile			Bar/trough Profile		
T_1	T_2	F_g	A_1	A_2	A_{BLW}	A_1	A_2	A_{BLW}
11.32	10.70	0.0051	0.4	0.12	0.00957	0.2	0.06	0.00239
11.44	10.60	0.0070	0.4	0.12	0.00958	0.2	0.06	0.00240
11.55	10.50	0.0086	0.4	0.12	0.00959	0.2	0.06	0.00240
11.69	10.40	0.0105	0.4	0.12	0.00962	0.2	0.06	0.00241
11.81	10.30	0.0124	0.4	0.12	0.00963	0.2	0.06	0.00241
11.94	10.20	0.0143	0.4	0.12	0.00965	0.2	0.06	0.00241
12.08	10.10	0.0162	0.4	0.12	0.00968	0.2	0.06	0.00242
12.15	10.05	0.0172	--	--	--	0.2	0.06	0.00242
12.22	10.00	0.0181	0.4	0.12	0.00970	0.2	0.06	0.00242
12.39	9.90	0.0204	0.4	0.12	0.00975	0.2	0.06	0.00244
12.54	9.80	0.0223	0.4	0.12	0.00978	0.2	0.06	0.00244
12.72	9.70	0.0245	0.4	0.12	0.00984	0.2	0.06	0.00246
12.88	9.60	0.0264	0.4	0.12	0.00988	0.2	0.06	0.00247
13.06	9.50	0.0286	0.4	0.12	0.00993	0.2	0.06	0.00248
13.26	9.40	0.0309	--	--	--	0.2	0.06	0.00250
13.48	9.30	0.0334	--	--	--	0.2	0.06	0.00252
13.69	9.20	0.0356	--	--	--	0.2	0.06	0.00254
13.90	9.10	0.0379	--	--	--	0.2	0.06	0.00256

Table 1. Parameters used for plane beach and bar/trough profile model runs. T_1 and T_2 are the incident wave periods (in sec.), f_g is the resulting group frequency (Hz), A_1 and A_2 are the incident wave amplitudes (m), and A_{BLW} is the boundary condition bound wave given by Ottesen Hansen et al. (1981) (m).

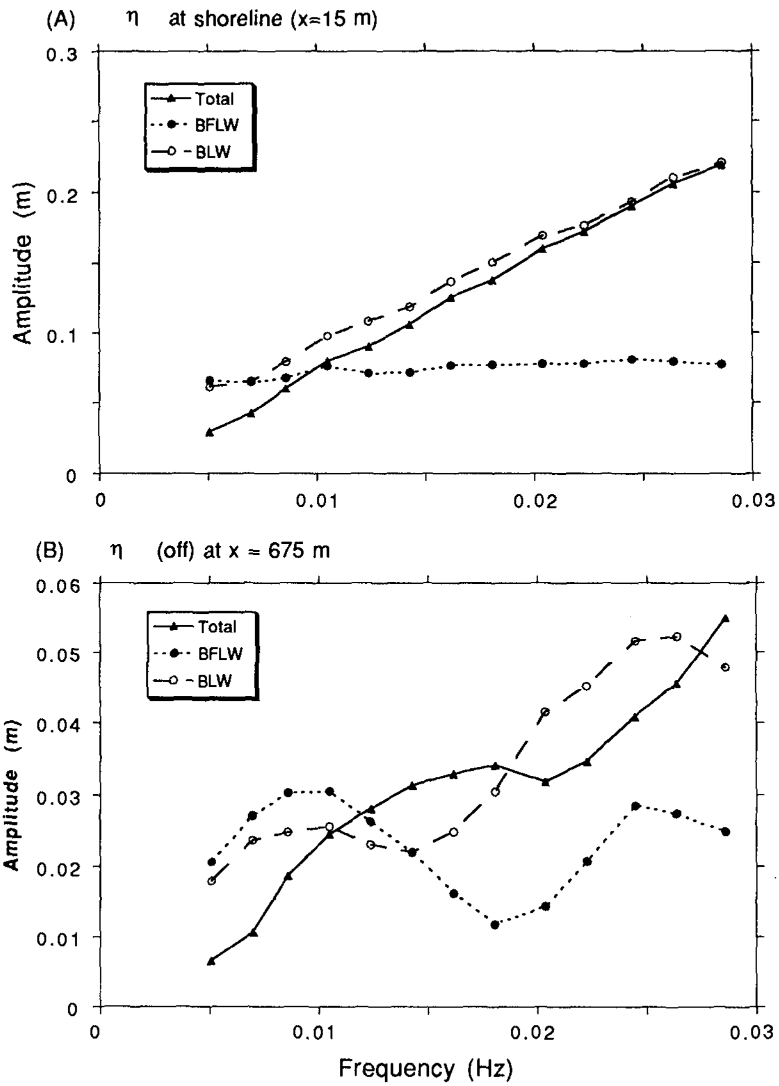

Figure 1. Model-generated long wave amplitudes of (A) η at the shoreline point of reflection and (B) offshore progressive component of η ($\eta(off)$) at $x = 675$ m over the profile shown in Fig. 2.

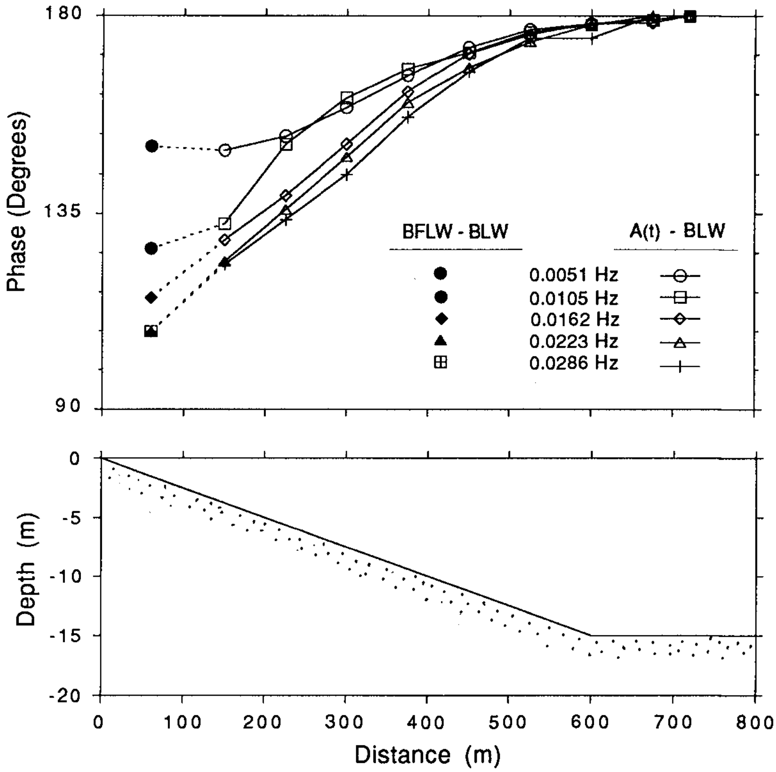

Figure 2. Phase between BFLW $\eta(on)$ and BLW $\eta(on)$ inside the surf zone (solid symbols) and between $A(t)$ and BLW $\eta(on)$ outside the surfzone (open symbols) for model-generated data at five group frequencies over the linear profile shown in the lower frame.

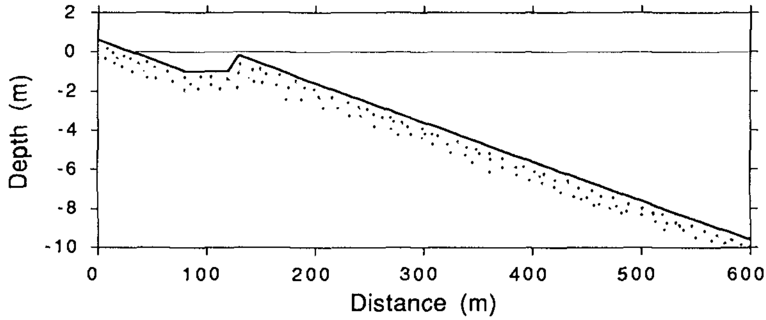

Figure 3. Bar/trough profile from Symonds and Bowen (1984). The profile used for model runs here (Figs. 4, 5) extends linearly to $h = -15$ m, where wave groups enter the model over a constant depth segment as in Fig. 2.

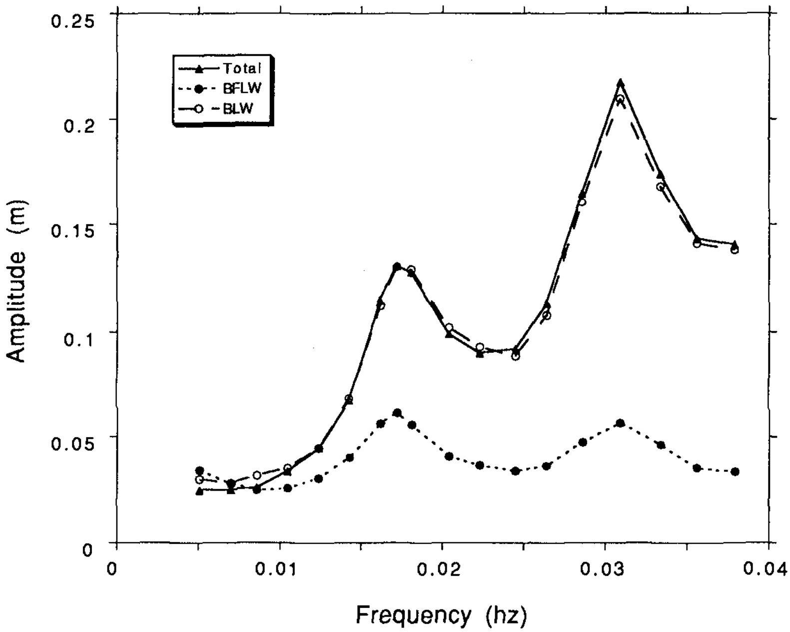

Figure 4. Model-generated long wave amplitudes of η at the shoreline point of reflection using the bar/trough profile (Fig. 3).

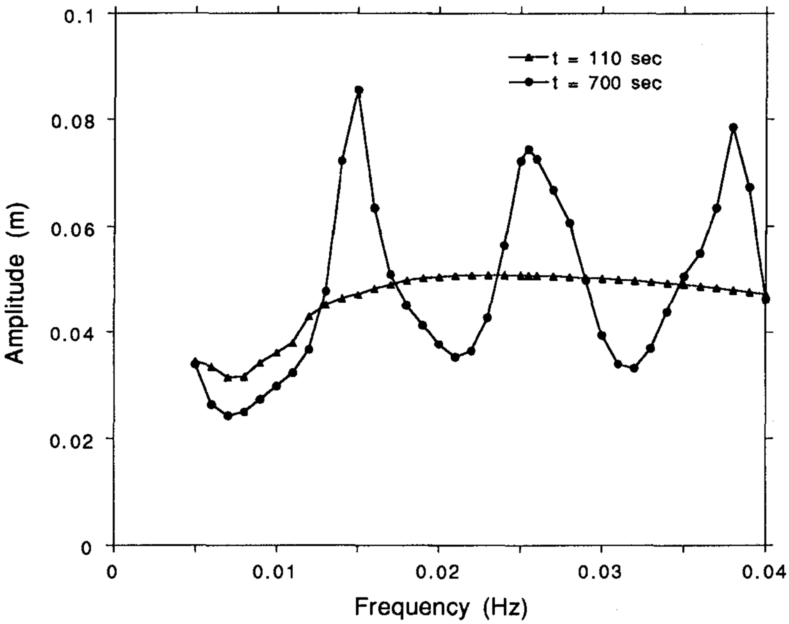

Figure 5. Model-generated long wave amplitudes of η at the shoreline point of reflection using the bar/trough profile. Incident wave forcing has been turned off and long waves are input at the offshore boundary at a series of discrete frequencies, each with $A = 0.01$ m. Long wave amplitudes were found by searching model-generated time series (obtained from independent model runs at each frequency) over an interval equal to the group period, T_g, starting at the times indicated.

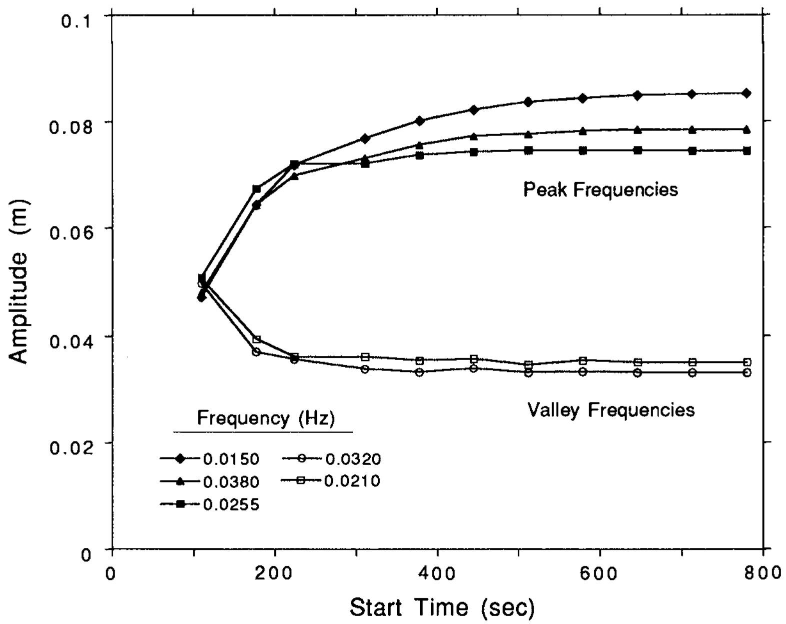

Figure 6. Time development of three peak and two valley amplitudes shown in Fig. 5. Start time refers to the time at the beginning of the interval, T_g, for finding amplitudes from model-generated time series.